Interaction of *Drosophila* Acetylcholinesterases with D-Tubocurarine: An Explanation of the Activation by an Inhibitor†

Marko Goličnik,‡ Didier Fournier,§ and Jure Stojan*,‡

Institute of Biochemistry, Medical Faculty, University of Ljubljana, Vrazov trg 2, 1000 Ljubljana, Slovenia, and Laboratoire d'Entomologie et Groupe de Chimie Biologie, Université Paul Sabatier, 31062 Toulouse, France

Received May 4, 2000; Revised Manuscript Received November 2, 2000

ABSTRACT: Homotropic cooperativity in *Drosophila melanogaster* acetylcholinesterase seems to be a consequence of an initial substrate binding to a high-affinity peripheral substrate binding site situated around the negative charge of D413 (G335, *Torpedo* numbering). An appropriate mutation which turns the peripheral binding site to a low-affinity spot abolishes apparent activation but improves the overall enzyme effectiveness. This contradiction can be explained as less effective inhibition due to a shorter occupation of such a peripheral site. A similar effect can be achieved by an appropriate peripheral inhibitor such as *TC*, which can in special cases, when less effective heterotropic inhibition prevails over homotropic, acts as an activator. At the highest substrate concentrations, however, these enzymes are always inhibited, although steric components may influence the strength of inhibition like in the F368G mutant (F290, *Torpedo* numbering). Cooperative effects thus may include a steric component, but covering of the entrance must affect influx and efflux to different extents.

Cholinesterases are serine hydrolases which fall broadly into two types depending on their substrate preference, susceptibility to inhibitors and tissue distribution. Acetylcholinesterases (AChEs,[1] EC 3.1.1.7) very effectively hydrolyze acetylcholine, and those which prefer larger choline esters are termed butyrylcholinesterases (BChE, EC 3.1.1.8) [for a review of cholinesterases, see Massoulié et al. (*1*)]. Insects possess only AChE situated only in the brain and which exhibits characteristics intermediate between those of vertebrate AChEs and BChEs (*2*, *3*).

Kinetic investigations and the resolved crystal structure of *Torpedo californica* and mouse AChEs (*4*, *5*) revealed at least two ligand binding sites on their active surface: CS, whose reacting residues are located some 20 Å deep inside the core of the molecule at the bottom of a narrow gorge, and PAS, composed of some residues at the entrance to this gorge (*6*, *7*). It appears that certain amino acid residues at the PAS may be important in catching and guiding the substrate molecules which enter the CS (*8*, *9*). The latter, in cholinesterases, consists again of two subsites: an "anionic" subsite where a positively charged substrate moiety binds and an "esteratic" subsite responsible for covalent catalytic hydrolysis of the substrate. The reaction mechanism, therefore, includes at least an initial reversible Michaelis complex formation, covalent acylation, and deacylation induced by a water molecule (*4*, *10*−*12*).

The kinetic behavior of cholinesterases from different sources deviates from the Michaelis−Menten pattern. These deviations are known as activation or inhibition at various substrate concentrations. Activation which is observed at intermediate substrate concentrations is followed by inhibition at the higher concentrations, as in the case of nematode and insect AChEs (*13*) or vertebrate BChEs (*14*). On the other hand, the only deviation from Michaelian kinetics in wild-type vertebrate AChEs is in the occurrence of the activity optimum at a substrate concentration of approximately 1 mM (*15*), but the extent of these phenomena differs in enzymes from different sources and especially in various mutated enzymes. Two main hypotheses have been proposed to explain the kinetic diversity of cholinesterases, yet both consider the unusual architecture of their active site. The first assumes a conformational modulation of the deacylation rate upon binding of an additional substrate molecule on the acyl−enzyme intermediate and vice versa (*16*), and the second involves purely steric obstruction of the products at the exit by the second substrate molecule bound to the PAS (*17*). The main objection to the first explanation is based on known three-dimensional structures of vertebrate AChE's complexes with inhibitors showing no significant intramolecular movements (*18*). However, our three-dimensional homology-built model (*19*) suggested and newly resolved crystal structure of the native *Dm*AChE (*20*) reveals such movements and therefore supports the first hypothesis.

Recently, a six-parameter kinetic model was introduced which is able to reproduce uniquely the initial rate, as well as progress curves data in wild-type *Dm*AChE (WT) or

† This work was supported by the Ministry of Science and Technology of the Republic of Slovenia (Grant P3-8720-0381) and by grants from DRET (94-084), IFREMER, and CNRS (GRD 1105 and ACS-SV3).

* To whom correspondence should be addressed: Institute of Biochemistry, Medical Faculty, University of Ljubljana, Vrazov trg 2, 1000 Ljubljana, Slovenia. Telephone: +386-61-5437651. Fax: +386-61-1320016. E-mail: stojan@ibmi.mf.uni-lj.si.

‡ University of Ljubljana.

§ Université Paul Sabatie.

[1] Abbreviations: AChE, acetylcholinesterase; BChE, butyrylcholinesterase; *ATCh*, acetylthiocholine; *TC*, D-tubocurarine; CS, catalytic site; PAS, peripheral anionic site; *Dm*AChE, AChE from *Drosophila melanogaster*.

10.1021/bi001024l CCC: $20.00
Published on Web 12/30/2000

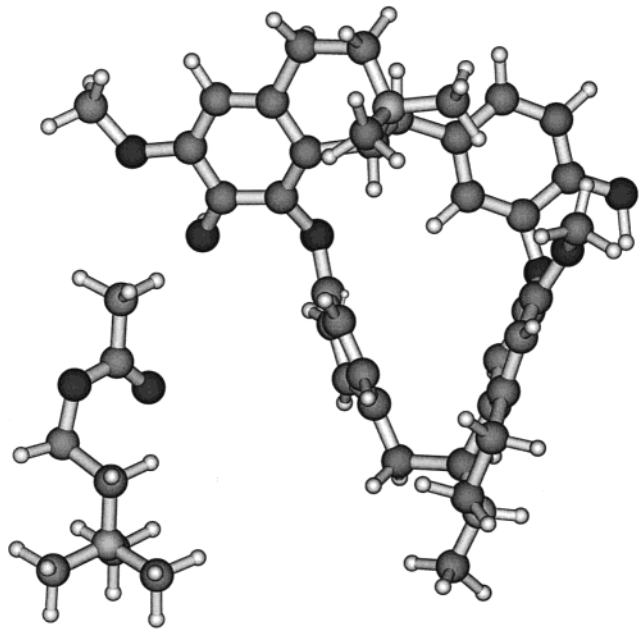

FIGURE 1: Ball and stick models of acetylcholine (left) and D-tubocurarine (right).

several mutated *Dm*AChEs (*21*, *22*). The model was operative also in the analysis of data in the presence of various reversible or irreversible active site-directed inhibitors (*23*, *24*). Moreover, the applicability to the kinetics of BChEs and in a simplified form for vertebrate AChEs was also verified.[2] The major objection to this model, however, is that it is empirical. In other words, one cannot assign each step in the model to the corresponding event in the catalytic process. To elucidate exactly this point, and especially the nature of activation−inhibition phenomena, we investigated the action of D-tubocurarine (Figure 1), a reversible peripheral ligand, on WT and on several different specifically site-mutated enzymes from *Drosophila melanogaster*.

EXPERIMENTAL PROCEDURES

Materials. Acetylthiocholine (*ATCh*) and 5,5-dithiobisnitrobenzoic acid (Ellman's reagent) were purchased from Sigma Chemical Co. (St. Louis, MO), and D-tubocurarine chloride (*TC*) was from Fluka Chemie AG (Buchs, Switzerland). Other substances were reagent grade. All experiments were carried out at 25 °C in 25 mM sodium phosphate buffer with an ionic strength of 44 mM and pH 7.

Truncated cDNA encoding soluble AChE of *D. melanogaster* was expressed with the baculovirus system (*25*). Secreted enzymes were purified and stabilized with 1 mg/mL BSA according to the method of Estrada-Mondaca and Fournier (*26*). Active site titration of the enzymes was carried out using 7-(methylethoxyphosphinyloxy)-1-methylquinolinium iodide (MEPQ) synthesized as described by Levy and Ashani (*27*). The residue numbering follows that of the precursor (*3*).

The hydrolysis of acetylthiocholine catalyzed by *Dm*AChEs was assessed in the absence and presence of *TC*, on a stopped-flow apparatus. Aliquots of two solutions, one containing only the enzyme and the other the substrate, *TC*, and Ellman's reagent were mixed together in the mixing chamber of the apparatus. The absorbency of the reaction mixture was recorded spectrophotometrically according to Ellman et al. (*28*) at various concentrations of the substrate and the inhibitor with a final concentration of the reagent of 1 mM. At low substrate concentrations, the reaction was followed until its completion, while at higher concentrations, only the initial portions were measured. To avoid possible product modulation or backward reaction, we stopped the measurement when 60 μM product was formed.

[2] J. Stojan, unpublished data.

Scheme 1

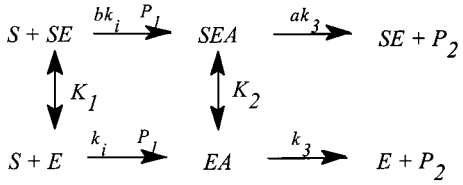

Scheme 2

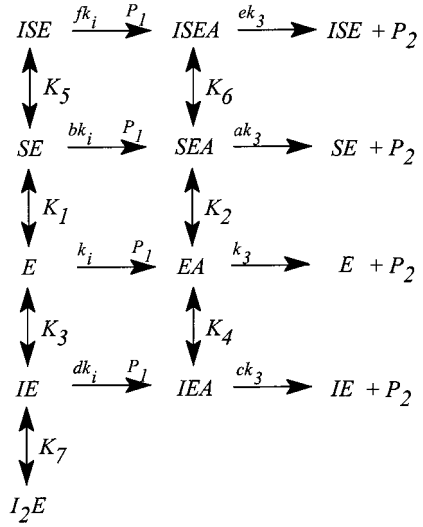

DATA ANALYSIS

For the analysis of progress curves in the absence of *TC*, we used the six-parameter model as presented previously (*21*, *22*) (Scheme 1).

In this scheme, *E* is the free enzyme, *EA* is the acylated enzyme, and *SE* and *SEA* represent the complexes with the substrate molecule bound at the modulation site. Products P_1 and P_2 are thiocholine and acetate, respectively.

A system of stiff differential equations which describe the model under combined steady-state and equilibrium assumptions (*23*) was fitted to the data of all experimental curves (13 curves, approximately 2500 points) simultaneously, using an appropriate computer program (*29*).

For the analysis of the experiments carried out in the presence of *TC*, we made an extension of the model to allow the binding of *TC* also with *SE* and *SEA* complexes. Additionally, we also included in the model a possible binding of another *TC* molecule (Scheme 2). In this scheme, *I* stands for *TC*.

The evaluation of corresponding kinetic parameters was carried out in two steps. (i) For the first estimation, a steady-state rate equation for the model in Scheme 2 was derived under the combined steady-state and equilibrium assumptions (*30*):

$$v_0 = \left[E_0 k_3 (S)\left(1 + a\frac{S}{K_2} + e\frac{SI}{K_2K_6} + c\frac{I}{K_4}\right)\right] / \left\{(S)\left(1 + \frac{S}{K_2} + \frac{SI}{K_2K_6} + \frac{I}{K_4}\right) + \left[k_3\left(1 + a\frac{S}{K_2} + e\frac{SI}{K_2K_6} + c\frac{I}{K_4}\right)\left(1 + \frac{S}{K_1} + \frac{SI}{K_1K_5} + \frac{I}{K_3} + \frac{I^2}{K_3K_7}\right)\right] / \left[k_i\left(1 + b\frac{S}{K_1} + f\frac{SI}{K_1K_5} + d\frac{I}{K_3}\right)\right]\right\} \quad (1)$$

The equation was fitted to the initial rates obtained from the progress curves in substrate hydrolysis measurements. (ii) The obtained parameters were used in the second step as initial estimates in fitting the numerically solved system of differential equations (cf. ref *23* and the Appendix) simultaneously to the complete set of progress curves (52 curves, approximately 10 000 points).

RESULTS

The progress curves for the hydrolysis of *ATCh* by W359L (W279, *Torpedo* numbering) mutant *Dm*AChE in the absence and presence of *TC* are shown in Figure 2. At low substrate concentrations, the curves reach the plateaus which correspond to each starting substrate concentration, and with increasing *TC* concentrations, these plateaus are achieved later. Thus, at low substrate concentrations, *TC* inhibits *ATCh* hydrolysis. The same effect is also evident when initial slopes of the corresponding progress curves are compared. On the other hand, the slopes of progress curves obtained with high substrate concentrations are the steepest in the presence of the highest *TC* concentrations (Figure 2D). This indicates that *TC* at high substrate concentrations acts as an activator.

Another representation of the same data is given in the form of theoretical *pS* curves in Figure 3B. It should be emphasized that the points in Figure 3 are numerical derivatives at time zero of each theoretical progress curve in Figure 2. Theoretical progress curves, again, were obtained by fitting differential equations for the model in Scheme 2 to all progress curves in Figure 2, simultaneously (see Data Analysis). The results of this fitting are presented in Table 1, and the corresponding parameters were put into eq 1 to calculate the curves in Figure 3.

Theoretical *pS* curves for WT, the D413G/F414L (G335 and Δ336, *Torpedo* numbering) mutant, and the F368G (F290, *Torpedo* numbering) mutant (Figure 3A,C,D), obtained by an analogues procedure (progress curves not given), show that in these enzymes *TC* inhibits *ATCh* hydrolysis at all tested substrate concentrations. There are, however, special characteristics evident from the shape of these *pS* curves: (i) the inhibition of the WT enzyme and the F368G mutant by *TC* is more effective than the inhibition of the D413G/F414L mutant; (ii) in the case of the F368G mutant, the curve with the highest *TC* concentration does not show inhibition at the highest substrate concentrations; (iii) the pattern of all curves for the D413G/F414L mutant resembles the pattern for vertebrate AChEs, indicating that this enzyme is not activated by the substrate at intermediate concentrations; and (iv) finally, it is a common tendency in Figure 3 that with increasing *TC* concentrations the "apparent" activation at intermediate substrate concentrations is less and less significant.

DISCUSSION

It seems that deviations from Michaelis−Menten kinetics are common to all cholinesterases, although they are sometimes not detectable; apparent activation at intermediate substrate concentrations is followed by various degrees of inhibition as we approach substrate concentrations close to maximal solubility. To describe such cooperativity in cholinesterases with a kinetic model, it must include two characteristics. The first is the well-evidenced existence of an acyl intermediate known from the molecular mechanism of catalysis (*4*, *10*−*12*). The second can be either the existence of multiple enzyme forms (*13*) or multiple-substrate binding of the substrate as the major mechanism underlying homotropic allosteric effects (*31*−*33*). Mathematically, the existence of multiple enzyme forms would result in summing up the needed number of Michaelis−Menten equations, but this possibility was rejected for *Dm*AChE (*13*, *34*). The simplest reasoning in the case of multiple-substrate binding would be to assign the interaction of one further substrate molecule to one deviation from Michaelian kinetics. It would lead to the conclusion that two substrate molecules interact with vertebrate WT AChEs, but the third one ought to be introduced with the WT *Drosophila* enzyme, nematode AChE, or various BChEs. The kinetic model in the latter case would be too complex to be evaluated from simple v versus [S] data. To reduce the complexity, one could make several kinetic parameters in the model equal; such an assumption would eliminate the allosteric component, thus exposing only steric effects (*17*). According to the resolved crystal structure, the simultaneous binding of three positively charged substrate molecules is very unlikely, since only half as much space as in *Torpedo* enzyme is available in the gorge of *Dm*AChE (*20*). But one can also assume that the additional binding of only one substrate molecule to a modulation site could mimic homotropic activation as well as inhibition (*21*, *22*).

It is well-evidenced in the literature that there is a peripheral substrate binding site in cholinesterases situated at the entrance to the active site (*4*−*7*, *35*, *36*). Therefore, we used D-tubocurarine, a potent charged inhibitor, to disturb the substrate interaction at this peripheral site. Additionally, we designed such site-specific mutated enzymes to eliminate either of the two characteristic phenomena: activation and inhibition.

It turned out that among numerous mutations at the rim of the active site, the D413G/F414L enzyme showed no activation, although it metabolized *ATCh* considerably more effectively than WT. It appears that the loss of a negative charge at the entrance enhances the enzyme action; the reason seems to be a drastic decrease in substrate affinity by the PAS for the free enzyme and, consequently, less stopping of the substrate while entering into the active site. The same pattern in the shape of the *pS* curve is characteristic for vertebrate AChEs with G335 and deletion at the positions homologous to D413 and F414, respectively. In human erythrocyte AChE, the substrate binding constant for the PAS and the substrate inhibition constant are very similar. So, it seems logical that instead of omitting the parameters K_1 and b (see Table 1) for the D413G/F414L mutant, they may be made equal to K_2 and 1, respectively. Setting b equal to 1, however, could either reflect unimpeded bypassing of the

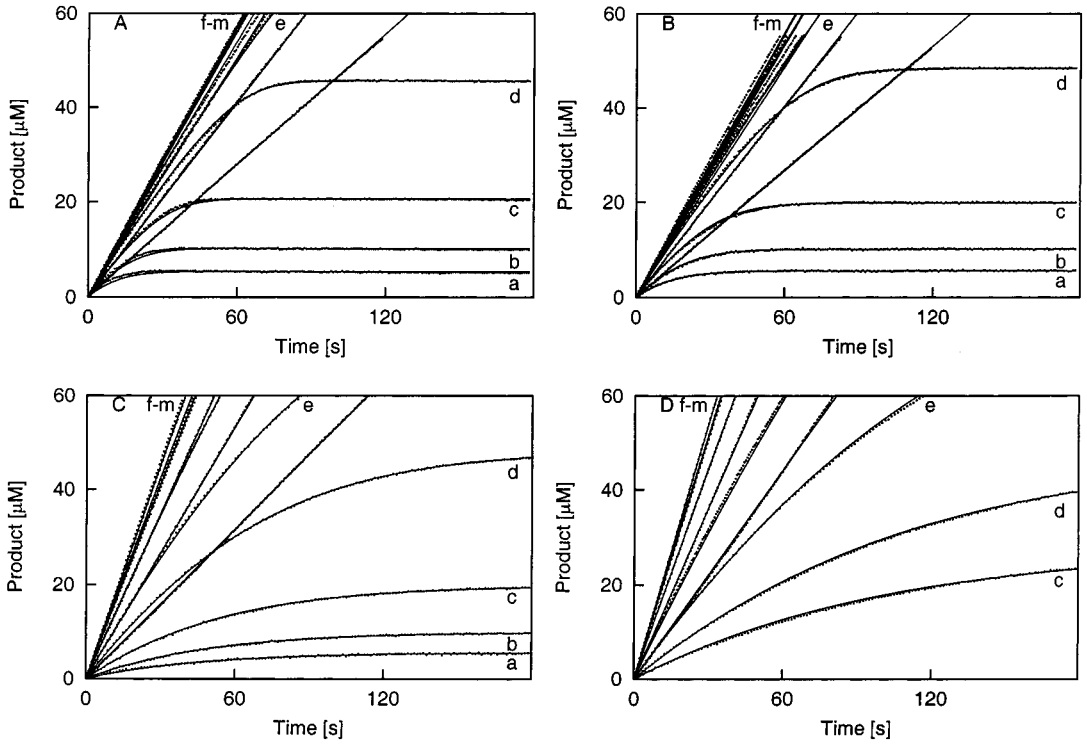

FIGURE 2: Progress curves for the hydrolysis of acetylthiocholine catalyzed by the W359L mutant of *D. melanogaster* AChE in the absence and presence of D-tubocurarine. In panels A and B the enzyme concentrations are 1.5 nM and in panels C and D 1.4 nM. Concentrations of D-tubocurarine are 0, 20 μM, 0.2 mM, and 0.5 mM in panels A−D, respectively. Substrate concentrations are from 5 μM to 50 mM.

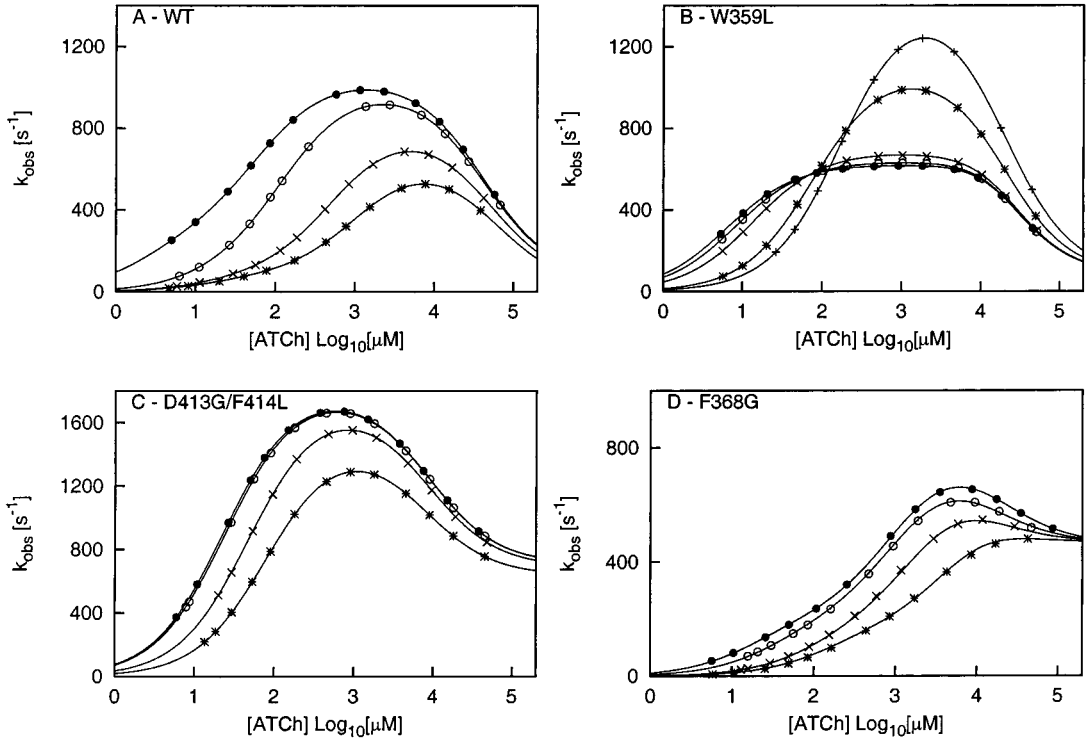

FIGURE 3: *pS* curves for the hydrolysis of acetylthiocholine catalyzed by various *D. melanogaster* AChEs in the absence and presence of D-tubocurarine. The concentrations of *TC* are (A) 0 (●), 2 μM (○), 20 μM (×), and 0.1 mM (*), (B) 0 (●), 5 μM (○), 20 μM (×), 0.2 mM (*), and 0.5 mM (+), (C) 0 (●), 1 μM (○), 20 μM (×), and 0.1 mM (*), and (D) 0 (●), 1.33 μM (○), 13.3 μM (×), and 66.6 μM (*).

substrate even if PAS is occupied or denote PAS as the initial binding site on the catalytic pathway.

The experiments carried out in the presence of *TC* with all tested enzymes reveal progressive vanishing of activation at intermediate substrate concentrations. Additionally, the affinity for *TC* (K_3) is strongly influenced by both mutations at the rim of the gorge (D413G/F414L and W359L), but the affinity for the substrate (K_1) is only influenced in the D413G/F414L mutant. If *TC* is too large to enter the active gorge, this indicates at least a partial overlap of binding surfaces for the substrate and *TC* with the D413-F414 site as a common point. We can summarize that the D413-F414

Table 1: Characteristic Constants for the Interactions of Various *Drosophila* Acetylcholinesterases with Acetylthiocholine and D-Tubocurarine[a]

	wild type	W359L	F368G	D413G/F414L
K_i	$1.1 \times 10^8 \pm 8 \times 10^6\ M^{-1}\ s^{-1}$	$8.23 \times 10^7 \pm 6 \times 10^6\ M^{-1}\ s^{-1}$	$1.23 \times 10^7 \pm 2 \times 10^5\ M^{-1}\ s^{-1}$	$8.19 \times 10^7 \pm 5 \times 10^5\ M^{-1}\ s^{-1}$
K_3	$978 \pm 1\ s^{-1}$	$5527 \pm 1\ s^{-1}$	$810 \pm 1\ s^{-1}$	$1804 \pm 2\ s^{-1}$
K_1	$4.16 \pm 0.01\ \mu M$	$8.79 \pm 0.08\ \mu M$	$2.22 \pm 0.05\ \mu M$	− or K_2[b]
K_2	24.1 ± 0.03 mM	2.29 ± 0.01 mM	17.8 ± 0.05 mM	8.68 ± 0.09 mM
a	0.067 ± 0.001	0.015 ± 0.001	0.056 ± 0.002	0.392 ± 0.001
b	0.193 ± 0.003	0.00040 ± 0.00001	0.098 ± 0.002	0 or 1[b]
K_3	$0.252 \pm 0.02\ \mu M$	$165 \pm 2\ \mu M$	$1.44 \pm 0.03\ \mu M$	$11.0 \pm 0.2\ \mu M$
K_4	$46.7 \pm 0.2\ \mu M$	$487 \pm 28\ \mu M$	$39.7 \pm 1.4\ \mu M$	0.462 ± 0.007 mM
c	0.365 ± 0.001	0.302 ± 0.016	0.478 ± 0.006	−
d	0.037 ± 0.006	0.884 ± 0.009	0.0741 ± 0.0010	0.148 ± 0.002
K_5	$1.16 \pm 0.2\ \mu M$	−	$15.2 \pm 0.2\ \mu M$	−
K_6	1.27 ± 0.07 mM	−	−	0.257 ± 0.017 mM
e	approaching zero	−	−	0.148 ± 0.012
f	0.00461 ± 0.00002	−	−	−
K_7	−	$32.1 \pm 0.2\ \mu M$	−	−

[a] −, not needed in the model. [b] Please see the text.

site is a primary high-affinity spot for charged ligands to contact *Dm*AChE. Since omitting it and switching to a low-affinity spot abolishes the substrate activation and enhance overall enzyme effectiveness, it seems that in enzymes with high-affinity PAS the apparent activation is in fact relatively effective substrate inhibition at intermediate substrate concentrations.

The *pS* curves for F368G (F290, *Torpedo* numbering) mutant (Figure 3D) are similar to the curves for WT. At intermediate substrate concentrations, there is an apparent activation and there is also inhibition by the excess of the substrate. However, from the pattern of the curves at the highest substrate concentrations, we can learn two things: (i) in contrast to other enzymes, a plateau is reached in the absence of *TC*, indicating a very weak substrate inhibition, and (ii) the convergence of all curves at this plateau reflects the competition between the substrate and *TC*. The weak substrate inhibition is expected for this mutant if we recall that at the homological position in BChE, phenylalanine is substituted with a smaller valine (V290, *Torpedo* numbering) (*37*), and that it has long been believed that there is no substrate inhibition with this enzyme. The competition between *TC* and the substrate at the highest concentrations indicates that substrate inhibition is probably caused by the same substrate molecule as the apparent substrate activation.

A very special case concerning substrate inhibition is the W359L mutant; in the absence of *TC*, we can see two peaks in the *pS* curve (Figure 3B). *TC* decreases the intensity of the peak at intermediate substrate concentrations but increases the intensity of the peak at high concentrations. It seems that the absence of bulky tryptophan at the rim of the gorge allows the binding of the second *TC* molecule (K_7). The substrate now competes with the two *TC* molecules, but it can also bypass the first one; in this case, heterotropic inhibition prevails until a sufficient substrate concentration is added. In this way, activation by *TC* is the consequence of inhibition by the first *TC* molecule that is less effective than substrate inhibition (*c* and $d > a$ and *b*).

The agreement between theoretical curves in all figures and the corresponding data indicates that the kinetic model in Scheme 2 is a very good mathematical explanation of our experiments. The model also suggests the binding of two *TC* molecules at the entrance of the active site, but only for the W359L mutant. Of course, we cannot exclude the same for WT and other mutants; however, the corresponding steps appeared to be unimportant in those enzymes and were therefore omitted (*38*). The findings are in agreement with previous reports on the multiple binding of *TC* on the electric eel enzyme where it was shown that the hydrolysis of various substrates is inhibited by *TC* with different inhibition constants (*39*). In the W359L mutant of *Dm*AChE, there is more space at the rim of the gorge and a substrate molecule could more easily pass into the gorge of the *IE* complex than with WT (compare the values of *d*). Consequently, the binding of another *TC* molecule might block completely the metabolization of *ATCh*. Interestingly, the lack of *ISE* and *ISEA* complexes in W359L also corroborates this explanation; the low substrate affinity at the PAS of the enzyme with bound *TC* allows its smooth entering and its immediate turnover. Thus, mathematically, K_5 and K_6 are compensated by $d \approx 1$ in the model. One could argue that K_5 and K_6 in fact represent the affinities of enzyme−substrate complexes for *TC*, but since the steps in the model that are connected with double arrows are treated under quasi-equilibrium assumptions, they also reflect affinities of enzyme−*TC* complexes for the substrate.

In this context, we discuss another virtual inconsistency of our six-parameter model, the great difference in the affinity constants between the free enzyme and the acyl−enzyme intermediate. We have shown that two putative peripheral site residues (D413 and F414) influence exactly these interactions. Their exclusion, by either mutation or covering, reduces the difference between the constants, and besides, the resolved crystal structures (*20*) display two different positions of F414 in the native enzyme and a third one in the complexes with inhibitors. Although the exact mechanism of these affinity switch remains open, the conformational changes are certainly involved.

Finally, we can summarize that our data on the action of *TC* on *ATCh* metabolization revealed substrate activation and inhibition as the same homotropic effect. Via comparison of the values of various dissociation and rate constants for different mutants, it seems that the binding area for the ligands may drastically change upon mutation, acylation, or binding of a homo- or heterotropic ligand. Cooperative effects may also include a steric component (see the F368G mutant), but the hindrance must affect, like in a wicker fish trap, entrances and exits to different extents.

APPENDIX

Derivation of Differential Equations for Scheme 2. The reaction presented by Scheme 2 in the text can be simplified:

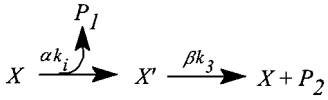

where $X = E + SE + IE + ISE + I_2E$ and $X' = EA + SEA + IEA + ISEA$.

Differential equations for the system described by the simplified scheme shown above are

$$\frac{dX}{dt} = -k_i\alpha(S)(X) + k_3\beta(X') \quad (2)$$

$$\frac{dS}{dt} = -k_i\alpha(S)(X) \quad (3)$$

$$\frac{dX'}{dt} = -k_i\alpha(S)(X) + k_3\beta(X') \quad (4)$$

$$\frac{dP_1}{dt} = k_i\alpha(S)(X) \quad (5)$$

$$\frac{dP_2}{dt} = k_3\beta(X') \quad (6)$$

where

$$\alpha = \frac{\left(1 + b\frac{S}{K_1} + d\frac{I}{K_3} + f\frac{SI}{K_1K_5}\right)}{\left(1 + \frac{S}{K_1} + \frac{I}{K_3} + \frac{SI}{K_1K_5} + \frac{I^2}{K_3K_7}\right)} \quad (7)$$

$$\beta = \frac{\left(1 + a\frac{S}{K_2} + c\frac{I}{K_4} + e\frac{SI}{K_2K_6}\right)}{\left(1 + \frac{S}{K_2} + \frac{I}{K_4} + \frac{SI}{K_2K_6}\right)} \quad (8)$$

REFERENCES

1. Massoulié, J., Pezzementi, L., Bon, S., Krejci, E., and Vallette, F. M. (1993) *Prog. Neurobiol. 41*, 31−91.
2. Hellenbrand, K., and Krupka, R. M. (1970) *Biochemistry 9*, 4665−4672.
3. Hall, L. M. C., and Spierer, P. (1986) *EMBO J. 5*, 2949−2954.
4. Sussman, J. L., Harel, M., Frolow, F., Oefner, C., Goldman, A., Toker, L., and Silman, I. (1991) *Science 253*, 872−878.
5. Bourne, Y., Taylor, P., and Marchot, P. (1995) *Cell 83*, 503−512.
6. Changeux, J. P. (1966) *Mol. Pharmacol. 2*, 369−392.
7. Taylor, P., and Lappi, S. (1975) *Biochemistry 14*, 1989−1998.
8. Botti, S. A., Felder, C. E., Lifson, S., Sussman, J. L., and Silman, I. (1999) *Biophys. J. 77*, 2430−2450.
9. Zhou, H., Wlodek, S. T., and McCammon, J. A. (1998) *Proc. Natl. Acad. Sci. U.S.A. 95*, 9280−9283.
10. Wilson, I. B., and Cabib, E. (1956) *J. Am. Chem. Soc. 78*, 202−207.
11. Quinn, D. (1987) *Chem. Rev. 87*, 955−979.
12. Barak, D., Kronman, C., Ordentlich, A., Ariel, N., Bromberg, A., Marcus, D., Lazar, A., Velan, B., and Shafferman, A. (1994) *J. Biol. Chem. 264*, 6296−6305.
13. Marcel, V., Palacois, L. G., Pertuy, C., Masson, P., and Fournier, D. (1998) *Biochem. J. 329*, 329−334.
14. Masson, P., Froment, M. T., Bartels, C., and Lockridge, O. (1996) *Eur. J. Biochem. 235*, 36−48.
15. Nachmanson, D. B., and Wilson, I. B. (1951) *Acta Enzymol. 12*, 259−339.
16. Eriksson, H., and Augustinsson, K. B. (1979) *Biochim. Biophys. Acta 567*, 161−172.
17. Szegletes, T., Mallender, W. P., and Rosenberry, T. L. (1998) *Biochemistry 37*, 4206−4216.
18. Harel, M., Schalk, I., Ehret-Sabatier, L., Bouet, F., Goeldner, M., Hirth, C., Axelsen, P. H., Silman, I., and Sussman, J. L. (1993) *Proc. Natl. Acad. Sci. U.S.A. 90*, 9031−9035.
19. Stojan, J. (1999) *J. Enzyme Inhib. 14*, 193−201.
20. Harel, M., Kryger, G., Rosenbery, T. L., Mallender, W. D., Lewis, T., Fletcher, R. J., Guss, J. M., Silman, I., and Sussman, J. L. (2000) *Protein Sci. 9*, 1063−1072.
21. Stojan, J., Marcel, V., Estrada-Mondaca, S., Klaébé, A., Masson, P., and Fournier, D. (1998) *FEBS Lett. 440*, 85−88.
22. Marcel, V., Estrada-Mondaca, S., Magné, F., Stojan, J., Klaébé, A., and Fournier, D. (2000) *J. Biol. Chem. 275*, 11603−11609.
23. Stojan, J., Marcel, V., and Fournier, D. (1999) *Chem.-Biol. Interact. 119−120*, 147−157.
24. Stojan, J., Marcel, V., and Fournier, D. (1999) *Chem.-Biol. Interact. 119−120*, 137−146.
25. Chaabihi, H., Fournier, D., Fedon, Y., Bossy, J. P., Ravallec, M., Devauchelle, G., and Cerutti, M. (1994) *Biochem. Biophys. Res. Commun. 203*, 734−742.
26. Estrada-Mondaca, S., and Fournier, D. (1998) *Protein Expression Purif. 12*, 166−172.
27. Levy, D., and Ashani, Y. (1986) *Biochem. Pharmacol. 35*, 143−146.
28. Ellman, G. L., Courtney, K. D., Andres, V., and Feathersone, R. M. (1961) *Biochem. Pharmacol. 7*, 88−95.
29. Stojan, J. (1997) *J. Chem. Inf. Comput. Sci. 37*, 1025−1027.
30. Cha, S. (1968) *J. Biol. Chem. 243*, 820−825.
31. Radic, Z., Reiner, E., and Taylor, P. (1991) *Mol. Pharmacol. 39*, 98−104.
32. Shafferman, A., Velan, B., Ordentlich, A., Kronman, C., Grosfeld, H., Leitner, M., Flashner, Y., Cohen, S., Barak, D., and Ariel, N. (1992) *EMBO J. 11*, 3561−3568.
33. Barak, D., Ordentlich, A., Bromberg, A., Kronman, C., Marcus, D., Lazar, A., Ariel, N., Velan, B., and Shafferman, A. (1995) *Biochemistry 34*, 15444−15452.
34. Estrada-Mondaca, S., Lougarre, S., and Fournier, D. (1998) *Arch. Insect Biochem. Physiol. 38*, 84−90.
35. Rosenberry, T. L. (1975) *Adv. Enzymol. Relat. Areas Mol. Biol. 43*, 103−218.
36. Berman, H. A., Becktel, W., and Taylor, P. (1981) *Biochemistry 20*, 4803−4810.
37. Harel, M., Sussman, J. L., Krejci, E., Bon, S., Chanal, P., Massouliè, J., and Silman, I. (1992) *Proc. Natl. Acad. Sci. U.S.A. 89*, 10827−10831.
38. Gibson, Q. (1983) Rapid Reaction Methods in Biochemistry, in *Modern Physical Methods in Biochemistry, Part B* (Neuberger, A., and Van Deenen, L. L. M., Eds.) pp 65−84, Elsevier Science Publications, Amsterdam.
39. Zorko, M., and Pavlic, M. R. (1986) *Biochem. Pharmacol. 35*, 2287−2296.

BI001024L